

Probing the Role of Protein Environment in Compound I Formation of Chloroperoxidase (CPO)

Marta Filizola and Gilda H. Loew*

Contribution from the Molecular Research Institute, 2495 Old Middlefield Way, Mountain View, California 94043

Received August 18, 1999. Revised Manuscript Received November 18, 1999

Abstract: Chloroperoxidase (CPO) is unique among the metabolizing heme proteins because it is a hybrid of two different families, peroxidases and cytochromes P450 (CYP450s). Unlike all other known peroxidases, with a conserved histidine as the proximal ligand of the heme iron, CPO has a cysteine ligand in common with the CYP450s. In addition, CPO can perform both peroxidase and CYP450 types of substrate oxidations. Despite these differences, the first steps of the CPO catalytic cycle are similar to those in the traditional heme peroxidases. Specifically, formation of the catalytically active Compound I species from the inactive ferric resting form proceeds via a transient peroxide complex. However, in CPO, the role of the protein environment in the distal peroxide binding site must be significantly different than that in typical peroxidases. This difference results from the presence of a unique glutamate residue instead of the two highly conserved residues, histidine and arginine, thought to be involved in Compound I formation of typical peroxidases. The goal of the computational studies presented here was to further elucidate the role of this unique glutamate residue, Glu 183, in transforming the transient peroxide intermediate to Compound I in CPO. Specifically, the proposed double role of Glu 183 in the CPO–HOOH complex first as a proton acceptor and then as a proton donor was investigated. The criteria used were the extent to which stable H bonds were formed between this unique residue and the peroxide ligand of the heme iron in the CPO–peroxide complex, during unconstrained MD simulations. Analysis of these simulations provided evidence for the double role of the Glu 183 first as proton acceptor and then as proton donor in CPO–Compound I formation from the peroxide intermediate.

Introduction

Chloroperoxidase (CPO), a secretory fungal heme peroxidase from *Caldariomyces fumago*, is unique in its ability to catalyze the hydrogen peroxide-dependent halogenation of aliphatic molecules, a process that gives rise to a wide variety of natural products, some of which like chloramphenicol are of medicinal value.¹ It also catalyzes other reactions characteristic of heme peroxidases (dehydrogenation), catalases (H₂O₂ dismutation), and cytochromes P450 (oxygen insertion).²

Comparison of the X-ray crystallographic structure of CPO,³ with other known peroxidases, namely cytochrome C peroxidase (CCP),⁴ ascorbate peroxidase (APX),⁵ lignin peroxidase (LiP),⁶ manganese peroxidase (MnP),⁷ fungal peroxidases from *Arthromyces ramosus* (ARP)⁸ and from *Coprinus cinereus* (CiP),⁹

peanut peroxidase (PNP),¹⁰ and horseradish peroxidase isoenzyme C (HRP–C),¹¹ reveals that CPO has none of the three key conserved residues found in both the proximal and distal regions of the heme unit in all the other peroxidases. Specifically, in CPO the proximal axial ligand of the heme iron is a mercaptide of a cysteine residue in common with the cytochromes P450 (CYP450s) but unlike the traditional heme peroxidases, which have a histidine residue as the proximal axial ligand. Moreover, neither the conserved His nor Arg, which are present in the distal binding site of the other eight peroxidases with a known structure, is found in CPO. Instead, a unique glutamate residue (Glu 183) is present in a similar but not identical position as the conserved His residue of traditional heme peroxidases. These structural features shared with both heme peroxidases and CYP450s make CPO the most versatile of the known heme enzymes.

Despite the differences in the proximal and distal regions of the heme unit, the enzymatically active form of CPO is the Compound I species (CPO-I), in common with all other peroxidases. Moreover, the pathway to formation of CPO-I from the inactive ferric resting state shown in Figures 1a–d is also very similar to that of typical peroxidases. In common with all peroxidases, this process requires stoichiometric amounts of hydrogen peroxide. As shown in Figure 1, the native enzyme, a ferric-aquo species (Figure 1a), is transformed by the addition of peroxide to a putative transient hydrogen peroxide complex (Figure 1b). This complex is then proposed to undergo protein-

* To whom correspondence should be addressed.

(1) Neidleman, S. L.; Geigert, J. In *Biohalogenation: Principles, Basic Roles, and Applications*; Ellis Horwood, Chichester, 1992.

(2) Griffin, B. W. In *Peroxidases in Chemistry and Biology*; Everse, J., Everse, K. E., Grisham, M. B., Eds.; CRC Press: Boca Raton, FL, 1992; Vol. II, pp 85–137.

(3) Sundaramoorthy, M.; Turner, J.; Poulos, T. L. *Structure* **1995**, *3*, 1367–1377.

(4) Poulos, T. L.; Freer, S. T.; Alden, R. A.; Edwards, S. L.; Skogland, U.; Takio, K.; Eriksson, B.; Xuong, N.; Yonetani, T.; Kraut, J. *J. Biol. Chem.* **1980**, *255*, 575–580.

(5) Patterson, W. R.; Poulos, T. L. *Biochemistry* **1995**, *34*, 4331–4341.

(6) Poulos, T. L.; Edwards, S. L.; Wariishi, H.; Gold, M. H. *J. Biol. Chem.* **1993**, *268*, 4429–4440.

(7) Sundaramoorthy, M.; Kishi, K.; Gold, M. H.; Poulos, T. L. *J. Biol. Chem.* **1994**, *269*, 32759–32767.

(8) Kunishima, N.; Fukuyama, K.; Matsubara, H.; Hatanaka, H.; Shibano, Y.; Amachi, T. *J. Mol. Biol.* **1994**, *235*, 331–344.

(9) Petersen, J. F. W.; Kadziola, A.; Larsen, S. *FEBS Lett.* **1994**, *339*, 291–296.

(10) Schuller, D. J.; Ban, N.; van Huystee, R. B.; McPherson, A.; Poulos, T. L. *Structure* **1996**, *4*, 311–321.

(11) Gajhede, M.; Schuller, D. J.; Henriksen, A.; Smith, A. T.; Poulos, T. L. *Nat. Struct. Biol.* **1997**, *4*, 1032–1038.

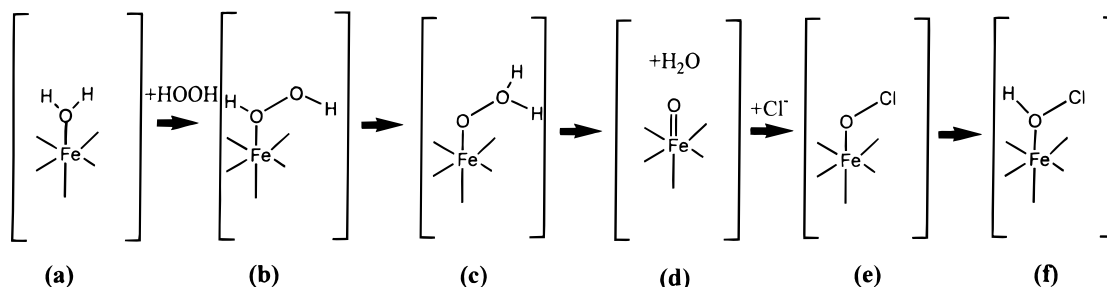


Figure 1. Proposed general reaction mechanism for chloroperoxidase-catalyzed reactions.

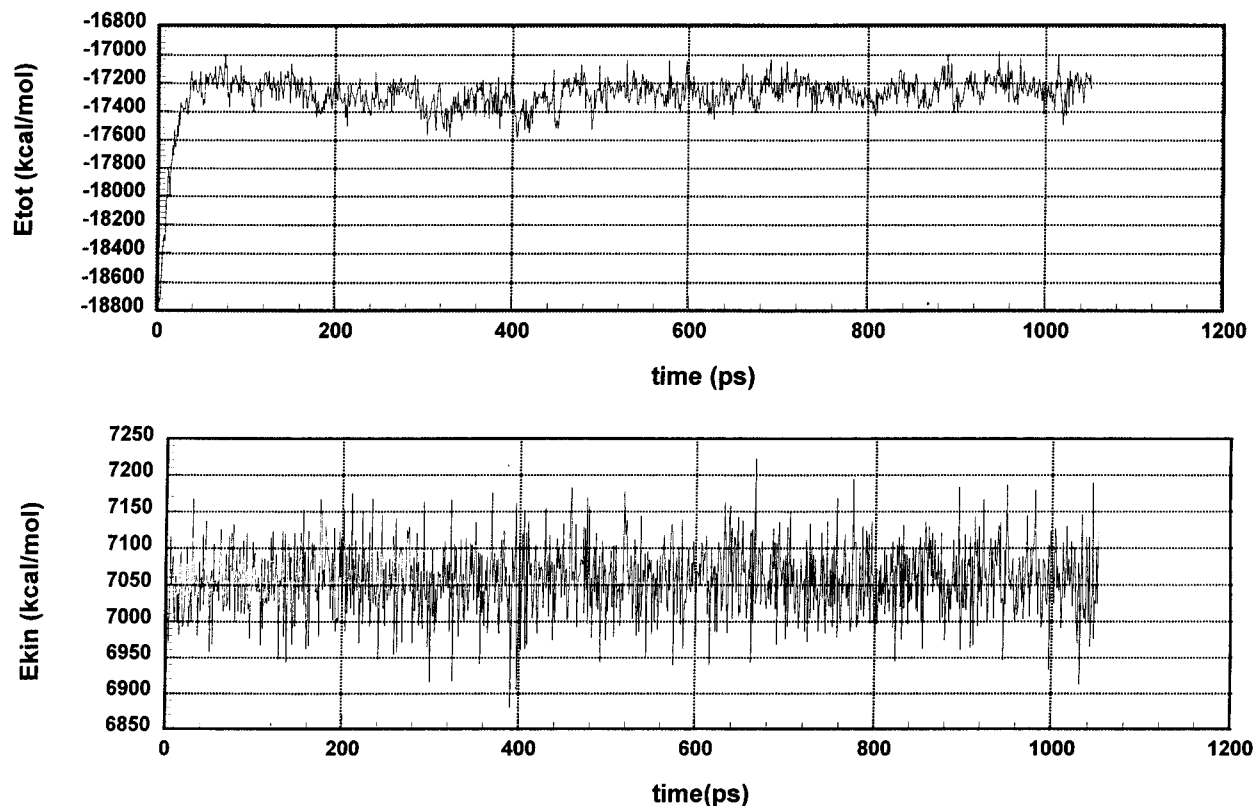


Figure 2. Total and kinetic energies during 1050 ps of MD simulations of CPO-HOOH.

assisted conversion to an oxywater complex (Figure 1c). This oxywater complex is then thought to undergo facile O–O bond cleavage leading to formation of water and Compound I (Figure 1d).

The second part of the enzymatic cycle, also shown schematically in Figure 1, is unique to CPO and involves dechlorination of substrates by CPO-Compound I. The mechanism of this reaction^{12–14} is still a subject of active experimental investigation. Figures 1e and 1f show a schematic representation of the most widely accepted mechanism. As indicated, Compound I is thought to abstract a chlorine atom from a substrate to form a hypochlorite intermediate (Figure 1e). This species is then thought to be protonated by a hydronium ion, which permits the formation of the intermediate shown in Figure 1f. The subsequent release of HOCl leads to the return of the enzyme to its resting state.

The computational study reported here focuses on further elucidation of the portion of the enzymatic cycle of CPO

common to all peroxidases, the formation of Compound I from the peroxide intermediate (Figures 1a–d). Specifically, the goal of the present work is to further elucidate the role of the unique Glu 183 in Compound I formation of CPO from the peroxide intermediate.

Previous studies¹³ based on the crystallographic structure of CPO³ already suggested a key role of Glu 183 in this pathway. Specifically, Glu 183 was proposed¹³ to play the double role of proton donor and proton acceptor to the peroxide ligand leading to Compound I formation. Although plausible, computational studies can be very useful for further assessment of this proposed role for the following reasons: (1) Deductions were made using the X-ray structure of the ferric-aquo resting form and not of the peroxide complex that is the essential precursor to Compound I. (2) The peroxide species is too transient for experimental structure determination. However, computational methods are ideally suited to characterize this transient intermediate using experimental information obtained for the more stable ferric form. (3) As is so far the case for proteins of this size, no hydrogen atoms are resolved in the X-ray structure. Yet, the mechanistic inference made using the X-ray structure invokes a key role for these missing H atoms. (4) The X-ray structure represents a static form of the enzyme corresponding to an

(12) Libby, R. D.; Beachy, T. M.; Phipps, A. K. *J. Biol. Chem.* **1996**, *271*, 21820–21827.

(13) Sundaramoorthy, M.; Turner, J.; Poulos, T. L. *Chem. Biol.* **1998**, *5*, 461–473.

(14) Wagenknecht, H. A.; Woggon, W. D. *Chem. Biol.* **1997**, *4*, 367–372.

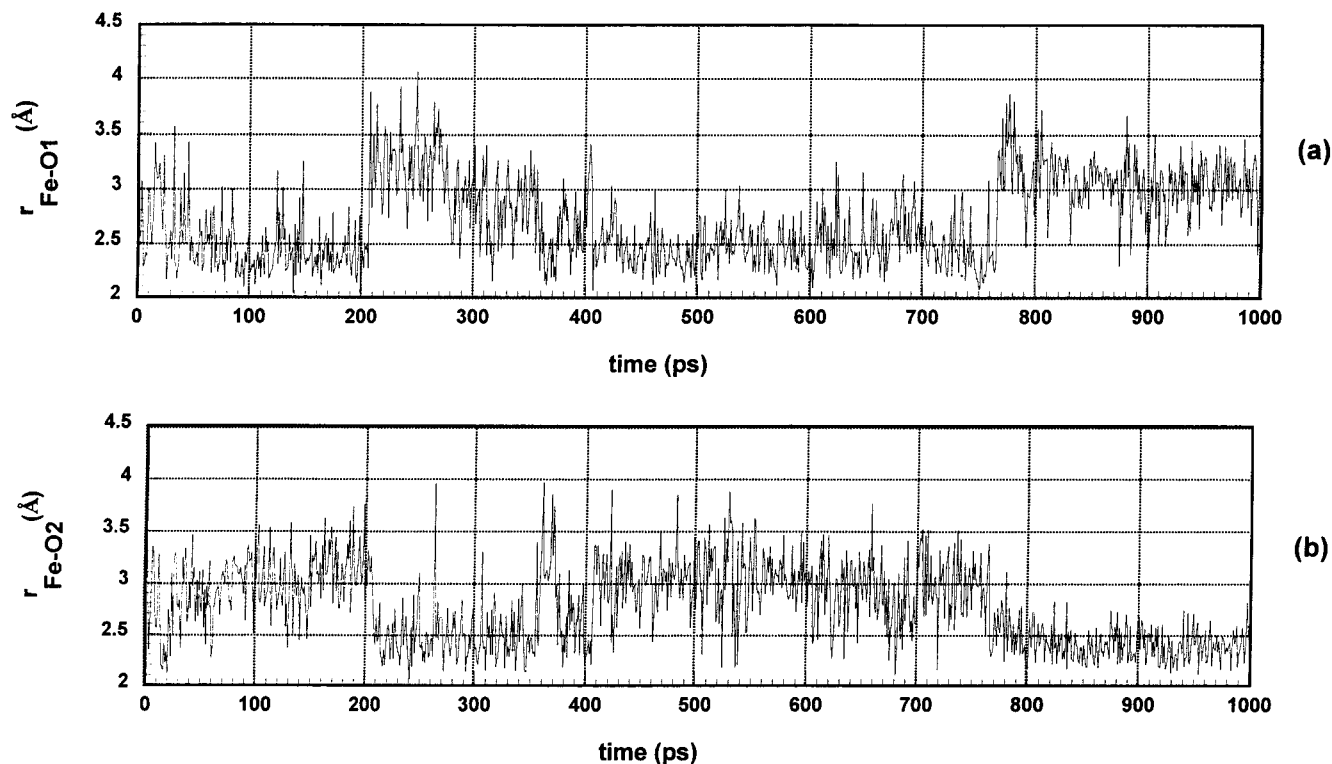


Figure 3. Distances calculated during the unconstrained MD simulations of 1 ns of CPO–HOOH between (a) the heme iron and the peroxide O1 and (b) the heme iron and the peroxide O2.

energetically stable form. To further probe the role of the protein environment in Compound I formation, the dynamic behavior of the protein could be important. Computational methods, using an X-ray structure, are ideally suited to provide this additional information.

In this work, the X-ray structure of the ferric-aquo CPO species was transformed to an initial structure of the ferric-peroxide CPO complex by adding peroxide as a ligand to the heme iron in a geometry determined from previous *ab initio* studies in our laboratory of a heme model for the HRP–HOOH complex.¹⁶ Although HRP and CPO differ in their proximal ligands, this difference is not expected to have a significant effect on the geometry of the peroxide ligand. Moreover, the initial CPO–HOOH complex formed was subjected to unconstrained energy minimization of the entire protein to allow possible peroxide geometry relaxation.

To explore an initial role of Glu 183 as a proton acceptor from the peroxide ligand, unconstrained full protein molecular dynamics simulations were performed for this transient CPO–peroxide complex, with Glu 183 in an anionic form. In addition, to explore the subsequent role of Glu 183 as a proton donor to the peroxide ligand, a second unconstrained MD simulation was performed for a second putative form of the transient species, with a neutral Glu 183 and an anionic species HOO^- as the ligand of the heme iron.

Analysis of the H-bonding interactions between nearby residues and bound water molecules of the CPO distal binding site monitored during these two unconstrained simulations provided evidence that Glu 183 plays a double role of proton

acceptor and proton donor, providing direct confirmation of the hypothesis based on crystallographic results.^{3,13}

Methods

The suite of programs embedded AMBER5.0¹⁵ was used for all calculations carried out in the present work. The CPO X-ray crystallographic structure³ including all crystallographic waters was used to dock the hydrogen peroxide ligand. Construction of the initial Fe–HOOH complex was guided by the optimized structure of a heme model peroxide intermediate of peroxidases previously determined in our laboratory by *ab initio* methods.¹⁶ Parameters for the hydrogen peroxide molecule were taken from these previous studies.¹⁶ Similarly, parameters for the anionic form of peroxide and the heme unit were taken from previous studies in our laboratory.¹⁷ The water molecule, which was the initial heme ligand at a distance of 3.2 Å from the iron in the crystallographic structure of the native enzyme, was not removed from the complex model. Instead, the initial complex was formed based on the assumption of a natural substitution reaction in which the peroxide takes the place of the water ligand. In addition to retaining all the crystallographic water molecules, a 7 Å solvent shell of water molecules was added around the X-ray crystallographic structure using the SOL option of AMBER. As a result, there are 1813 noncrystal solvent molecules in the system studied.

Energy minimization of the two different forms of the CPO–peroxide complex considered was carried out in two steps, both using a dielectric constant $\epsilon = 1$ and a cutoff of 13 Å. The purpose of the first step was to reorient the water molecules in the electric field of the system. Accordingly, the complex with all heavy atoms constrained by a harmonic constraint of 10 kcal/Å² was subjected to 2000 cycles of steepest descent followed by the conjugate gradient method until the rmsd between the structures of two consecutive iterations was less than 0.1 Å. In the second step, unconstrained minimization was carried out using the same procedure reported above.

MD simulations were carried out using the resulting energy minimized structures of each of the two forms of the CPO–peroxide complex as a starting point. A dielectric constant $\epsilon = 1$ was used and the nonbonded interactions were truncated at the relatively long distance of 13 Å. The nonbonded pair list was updated every 10 steps. A four-

(15) Cornell, W. D.; Cieplak, P.; Bayly, C. I.; Gould, I. R.; Merz, K. M., Jr.; Ferguson, D. M.; Spellmeyer, D. C.; Fox, T.; Caldwell, J. W.; Kollman, P. A. *J. Am. Chem. Soc.* **1995**, *117*, 5179–5197.

(16) Loew, G.; Dupuis, M. *J. Am. Chem. Soc.* **1996**, *118*, 10584–10587.

(17) Harris, D. L.; Loew, G. H. *J. Am. Chem. Soc.* **1996**, *118*, 6377–6387.

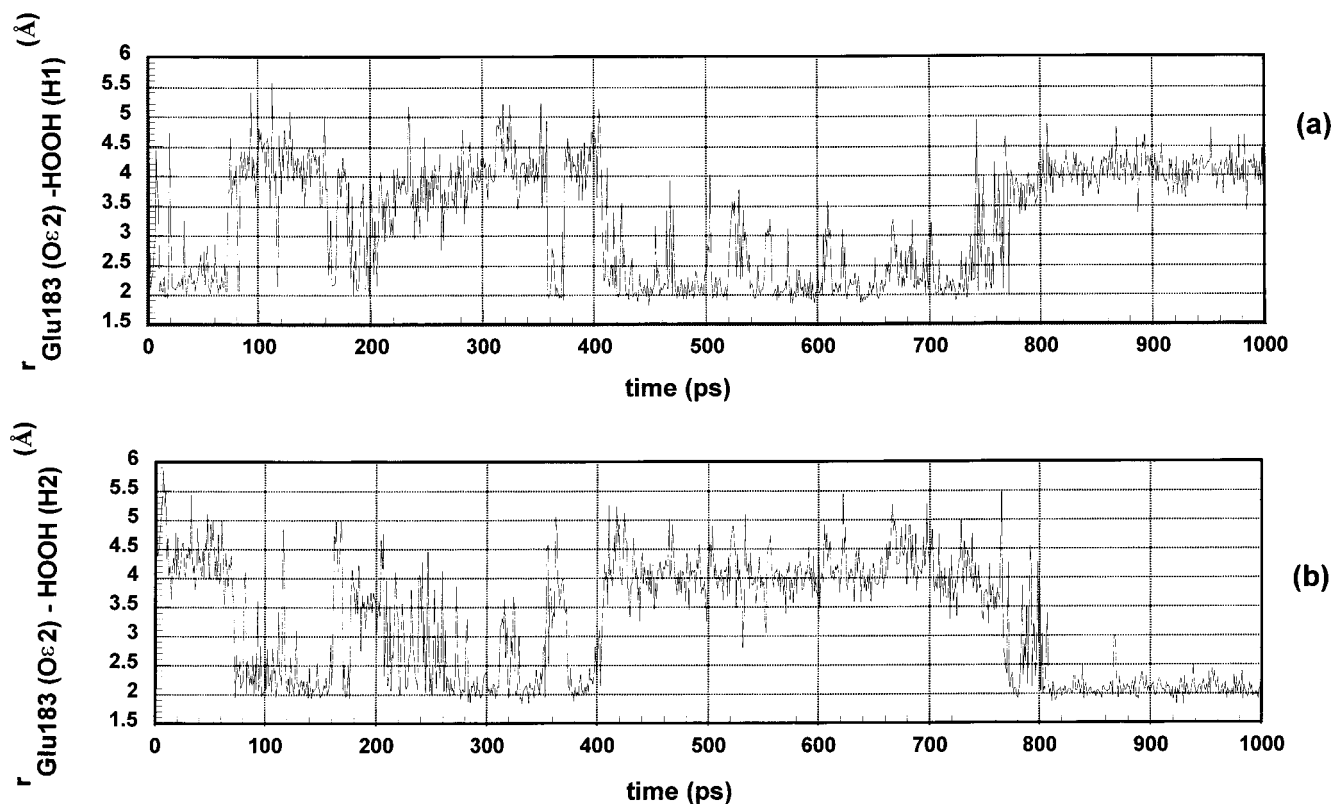


Figure 4. Distances calculated during the unconstrained MD simulations of 1 ns of CPO–HOOH between (a) the $O_{\epsilon 2}$ atom of the Glu 183 side chain and the peroxide H1 and (b) the $O_{\epsilon 2}$ atom of the Glu 183 side chain and the peroxide H2.

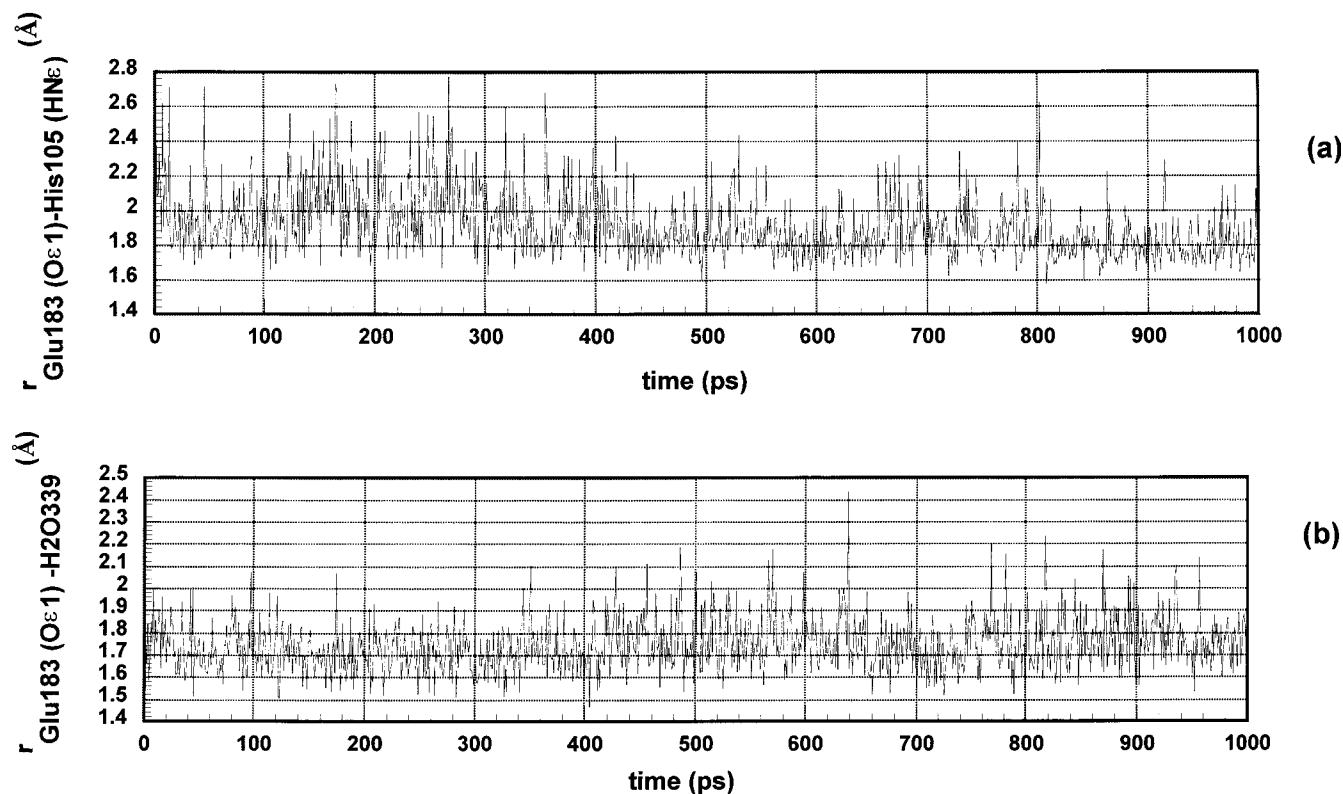


Figure 5. Distances calculated during the unconstrained MD simulations of 1 ns of CPO–HOOH between (a) the $O_{\epsilon 1}$ atom of the Glu 183 side chain and the HNe atom of the cationic His 105 and (b) the $O_{\epsilon 1}$ atom of the Glu 183 side chain and a hydrogen of the crystallographic water molecule H_2O_{339} .

stage heating procedure was performed. First, all atoms in the system were constrained with a harmonic constraint of $10 \text{ kcal}/\text{\AA}^2$ for 1 ps, using a 300 K initial velocity distribution. Second, the harmonic force constant was reduced to $5 \text{ kcal}/\text{\AA}^2$ and the run was continued for another

1 ps, using the final velocities of the first step. In step 3, the simulations were continued for 2 ps with a reduced harmonic force constant of $1.0 \text{ kcal}/\text{\AA}^2$. Finally, in step 4, the harmonic force constant was reduced to $0.5 \text{ kcal}/\text{\AA}^2$ for another 2 ps. At the end of heating, all constrained

were removed with the exclusion of a harmonic constraint of 0.1 kcal/Å² to the oxygen atoms of the noncrystallographic water molecules. The reason for keeping the oxygen atoms of the shell water molecules under a very small constraint was to prevent them from completely evaporating, while allowing them to move large distances. Using these conditions, equilibration was achieved in 50 ps for the MD simulations of the two different forms of the CPO–peroxide complex. After equilibration, production runs of 1 ns were carried out. Coordinates were saved for further analysis along the entire equilibrated trajectories.

Results and Discussion

Assessment of the Role of the Anionic Glu 183 as a Proton Acceptor from the Peroxide Ligand in CPO Compound I Formation. Figure 2 shows the total and kinetic energies calculated during 1050 ps of MD simulations carried out using the energy-minimized CPO–HOOH complex with the anionic form of Glu 183. As can be seen in this figure, equilibration was achieved after 50 ps and the complex was energetically stable during the entire unconstrained MD simulations of 1 ns. The rms deviation between all heavy atoms of the CPO structure obtained at the end of the unconstrained MD simulation and those of the crystal structure was 1.4 Å, indicating that the three-dimensional protein structure is conserved during the simulation.

The mode of binding of peroxide to the heme iron of CPO was determined by monitoring the Fe–O1 and Fe–O2 distances during the unconstrained MD simulation of 1 ns. The results are shown in Figure 3a,b. As shown in this figure, the peroxide binds primarily in an end-on fashion but with alternating domains during the MD trajectory in which either the peroxide oxygen atom O1 or the peroxide oxygen atom O2 can be ligands to the heme iron. At the beginning of the simulations (0–400 ps) there is a rapid exchange between the peroxide O1 (Figure 3a) and O2 (Figure 3b) as ligands for the heme iron. This is followed by two more well-defined domains of longer duration in each of which either the O1 (400–765 ps) or the O2 (765 ps–1 ns) is clearly the only ligand for the iron. The finding that one or the other peroxide oxygen atom is always a ligand for the heme iron with a distance of about 2.5 Å indicates the formation of a stable complex, even with no a priori imposition of a formal bond between the iron and the peroxide oxygen.

The MD trajectory was analyzed to identify robust H-bonding interactions of the peroxide with its surrounding distal residues and bound waters. The presence and nature of such stable H-bonding interactions was the main property used to assess the role of the protein environment in Compound I formation of CPO. The results of this analysis indicate that during the entire 1 ns of unconstrained MD simulations, the anionic Glu 183 is the only distal residue that maintains a stable interaction with the peroxide ligand. Moreover, there are no crystallographic water molecules in the distal binding site of CPO that maintain stable interactions with the peroxide ligand during the entire MD simulation of 1 ns. Nor is any other residue linked to the peroxide ligand by a stable H-bonding network. Thus Glu 183 is the only distal residue that can act as a proton acceptor from the peroxide ligand. These results are shown in Figures 4a and 4b.

The detailed analysis of the manner in which the carboxylate oxygen atom O_e2 of Glu 183 interacts with the peroxide ligand (Figures 4a and 4b) provides further direct support for the proposed role of Glu 183 as a proton acceptor from the proximal hydrogen atom of the peroxide ligand. Comparison of Figures 3a,b with 4a,b shows that the Glu 183 O_e2 oxygen interacts with whichever hydrogen of the peroxide is bound to the proximal oxygen atom. This behavior is most clearly demonstrated in the 400–1000 ps portion of the simulation. Specif-

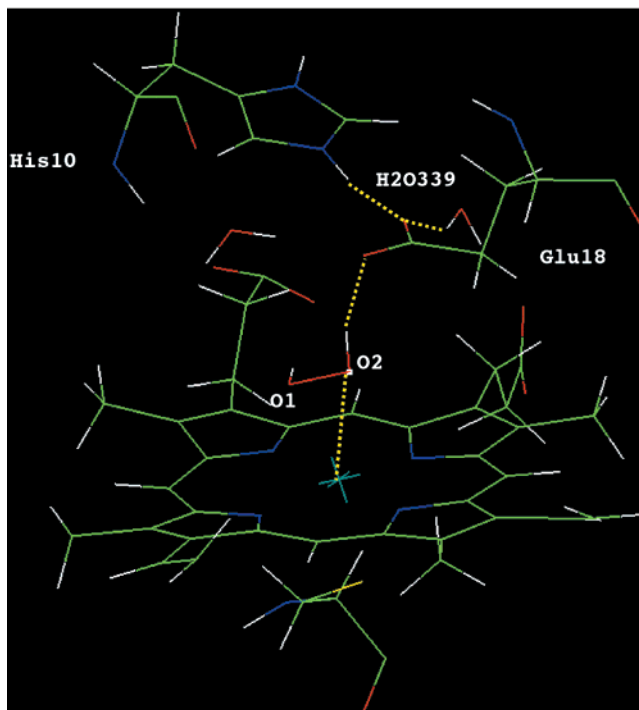
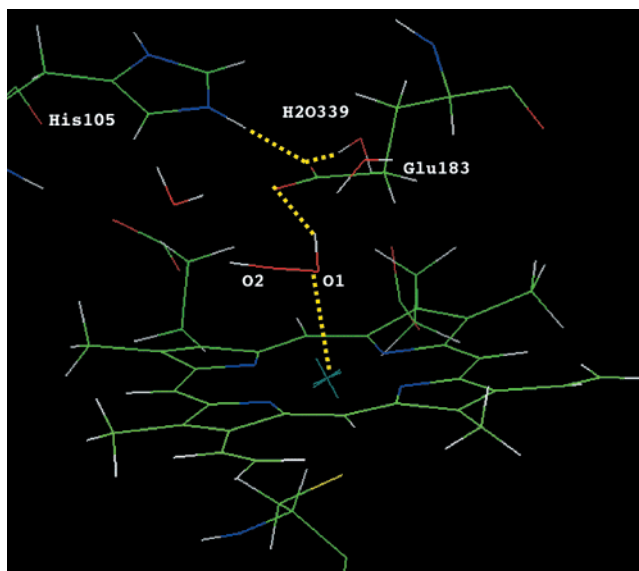


Figure 6. Typical snapshots of the distal binding pocket of the CPO–HOOH complex representative of the two different binding modes of peroxide with O1 (a) or O2 (b) as ligands for the heme iron.

ically, in the interval from 400 to 765 ps, where the peroxide oxygen atom O1 is the ligand for the heme iron (Figure 3a), the peroxide hydrogen H1 forms a stable H bond with the O_e2 atom of Glu 183 (Figure 4a). Similarly, when O2 is the peroxide ligand to the iron, i.e., from 765 ps to 1 ns (Figure 3b), the peroxide hydrogen atom H2 is the one that interacts with the O_e2 atom of Glu 183 (Figure 4b).

Another important deduction that can be made from the MD simulation is the manner in which the other carboxylate oxygen of Glu 183, O_e1, interacts with its immediate environment. Although it does not interact with the peroxide ligand, the O_e1 of Glu 183 finds other favorable partners in the immediate environment of the distal binding site. As shown in Figures 5a and 5b, during the entire 1 ns of unconstrained MD simulations, the carboxylate O_e1 atom of the Glu 183 side chain is involved in two stable interactions. One is a salt bridge formed between

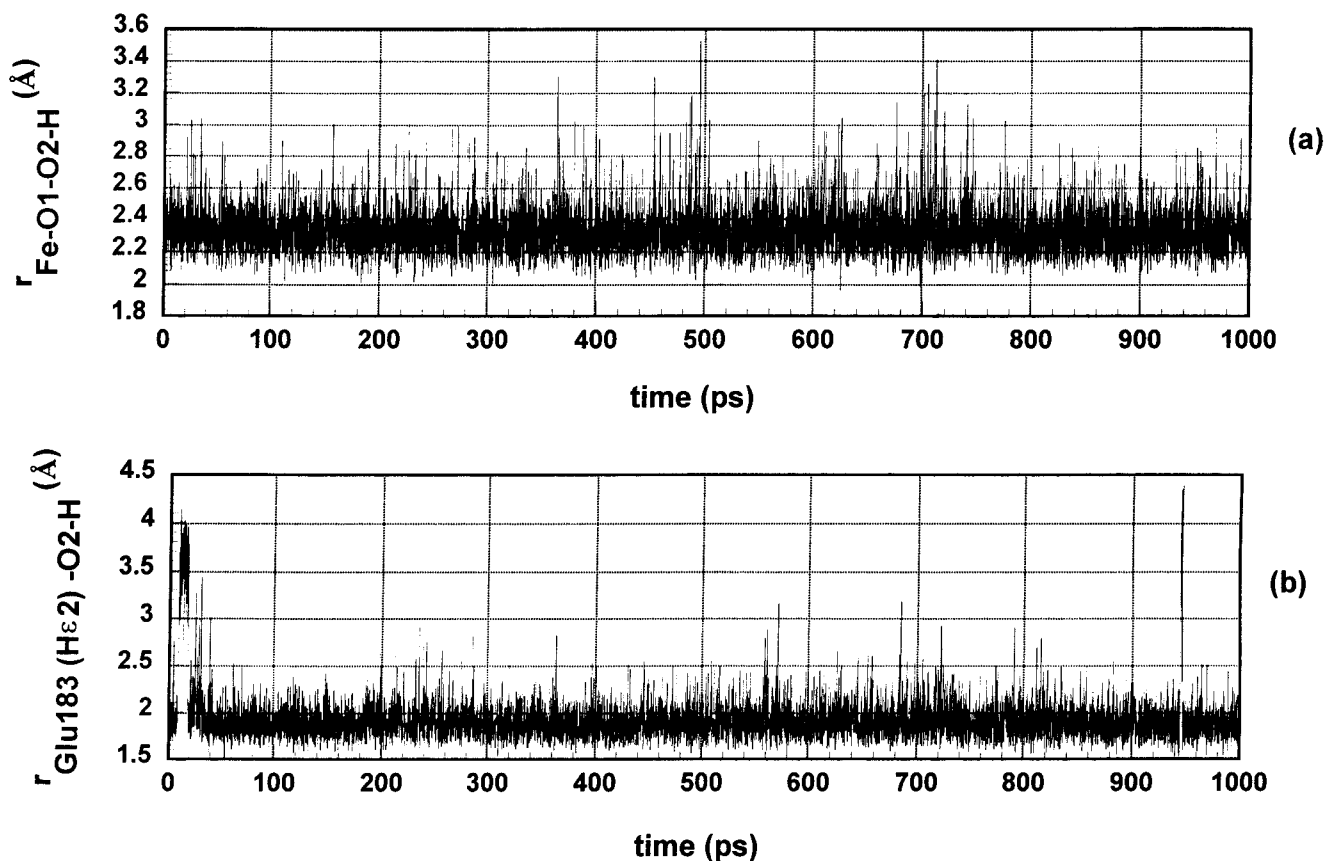


Figure 7. Distances calculated during the unconstrained MD simulations of 1 ns of the CPO–OOH[−] complex with Glu 183 in its neutral form, between (a) the peroxide proximal oxygen and the heme iron and (b) the He2 atom of the neutral Glu 183 and the distal peroxide oxygen.

the HN ϵ atom of the cationic His 105 and the carboxylate O ϵ 1 atom of the Glu 183 (Figure 5a). The other is an H bond of the same carboxylate O ϵ 1 atom with a hydrogen of the crystallographic water molecule H₂O₃₃₉ (Figure 5b). The formation of the stable salt bridge rules out a direct role for either partners, the HN ϵ atom of His 105 and the carboxylate O ϵ 1 atom of Glu 183, in Compound I formation. However, this strong interaction involving O ϵ 1 helps to firmly orient the other carboxylate oxygen, O ϵ 2, in a favorable position for H bonding to the proximal H of the peroxide ligand.

Figure 6a shows a typical snapshot of the distal binding pocket of the CPO–HOOH complex in the domain of the MD trajectory, when O1 is the ligand atom. Shown in this figure is the stable H bond found between the O ϵ 2 atom of Glu 183 and the hydrogen on the peroxide oxygen directly bound to the heme iron.

Figure 6b shows a typical snapshot of the distal binding pocket of the CPO–HOOH complex in the alternative domain of the MD trajectory, when O2 is the ligand atom. Again, as seen in this figure, the O ϵ 2 atom of Glu 183 forms a stable H bond with the hydrogen of the peroxide oxygen bound to the heme iron.

Also indicated in Figures 6a and 6b are the stabilizing interactions between the O ϵ 1 atom of the Glu 183 and two partners: (i) the HN ϵ atom of the cationic His 105 and (ii) a hydrogen of the crystallographic water molecule H₂O₃₃₉.

The formation of a stable H bond between the O ϵ 2 atom of Glu 183 H and the hydrogen of the peroxide oxygen bound to the heme iron, shown in Figures 6a and 6b, is indicative of facile transfer of the proximal proton from the peroxide ligand to the O ϵ 2 atom of Glu 183, and thus supports the postulated initial role of Glu 183 as a proton acceptor.

The consequence of this postulated proton transfer is a neutral form of Glu 183 and an anionic form (HOO[−]) of the peroxide ligand. Thus, this form of the complex was further investigated for the plausibility of the subsequent role of the neutral Glu 183 as a proton donor to the peroxyanion ligand.

Assessment of the Role of the Neutral Glu 183 as a Proton Donor to the Peroxyanion Ligand in CPO Compound I Formation. The Fe–OOH[−] form of the transient CPO–peroxide intermediate with a neutral Glu 183 was constructed to investigate the role of the neutral Glu 183 as a proton donor to the peroxyanion ligand in CPO Compound I formation. This complex was then subjected to energy minimization and 1 ns of unconstrained MD simulations, using the procedure described in the methods section.

Support for structural stability during 1 ns of unconstrained MD simulations is given from the small rmsd value of 1.5 Å obtained after superimposition between all heavy atoms of the enzyme at the end of the unconstrained MD simulations and those of the initial energy minimized structure.

As shown in Figure 7a, during the entire simulation the anionic oxygen of the HOO[−] species remains as a ligand to the heme iron.

The MD trajectory was analyzed to identify robust H bonding interactions of the peroxyanion with its surrounding distal residues and bound waters. Analysis of the H bonding interactions of the hydrogen peroxide ligand with the nearby neutral Glu 183 residue as well as with the crystallographic water molecules during the MD simulation led to the identification of stable H bonds between the He2 atom of Glu 183 and the distal oxygen of the peroxyanion. Figure 7b shows this important hydrogen bond between the He2 atom of the neutral Glu 183

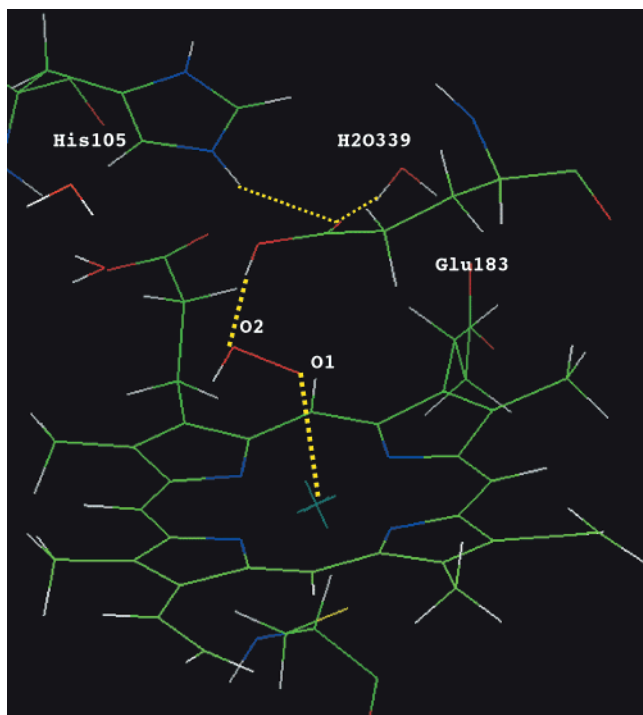


Figure 8. Typical snapshot of the distal binding site of the CPO-OOH⁻ neutral Glu 183 complex, during the entire 1 ns of unconstrained MD simulations.

and the distal peroxide oxygen that is stable during the entire nanosecond of unconstrained MD simulations.

Figure 8 is a typical snapshot of the distal binding pocket during this trajectory. It shows the stable H bond found between the H ϵ_2 of Glu 183 and the distal O 2 atom of the peroxide. Also indicated in this figure are the stabilizing interactions between the O ϵ_1 atom of the Glu 183 and two partners: (i) the H δ_1 atom of the cationic His 105 and (ii) a hydrogen of the crystallographic water molecule H $_2$ O $_{339}$. These interactions are maintained during this unconstrained MD trajectory as well.

These results taken together clearly support a role for the neutral Glu 183 as proton donor to the distal oxygen of the peroxide, leading to the formation of the oxywater complex thought to be required for Compound I formation.

Conclusions

The main goal of this computational study was to further explore the postulated double role of the unique distal Glu 183 residue, first as proton acceptor and then as proton donor, in

CPO Compound I formation. To this end, MD simulations of the CPO-HOOH complex with an anionic Glu 183 were performed to assess the role of Glu 183 as proton acceptor. In addition, MD simulations of the CPO-OOH⁻ complex with a neutral Glu 183 were performed to assess its subsequent postulated role as proton donor. The combined results of these simulations provide evidence for a dual role of the distal Glu 183 consistent with a previous hypothesis¹³ based on crystallographic results.³

The stable H bond maintained during the entire simulation of the CPO-HOOH complex with an anionic Glu 183 allows the inference that the O ϵ_2 atom of the anionic Glu 183 can act as a proton acceptor of the H atom on the proximal oxygen atom of the peroxide. During subsequent MD simulations of the CPO-OOH⁻ complex with a neutral Glu 183, the stable hydrogen bond formed between the H ϵ_2 atom of the neutral Glu 183 and the distal oxygen atom of the peroxyanion ligand allows the inference that the H ϵ_2 atom of the neutral Glu 183 can act as a proton donor to this distal oxygen atom. These two sequential steps lead directly to the oxywater species, allowing facile formation of Compound I and water.

This result for CPO reported here together with a recent similar study for the typical peroxidase HRP-C¹⁸ clearly indicate how Glu 183 can take the place of the conserved His 42 and Arg 38 in the distal binding site of the more typical peroxidases. In that study,¹⁸ it was found that His 42 cannot play the role of both proton donor and acceptor. His 42 can act as proton acceptor and Arg 38 as donor in either a sequential or simultaneous fashion to form the oxywater species. By contrast, the single Glu 183 can play the role of both proton acceptor and donor in the CPO distal binding site. This proposed mechanism clearly implies a two-step sequential pathway to formation of the oxywater complex, involving two forms of the peroxide intermediate of CPO, CPO-HOOH, and CPO-OOH⁻. Further experimental studies using the stopped flow spectroscopic method are suggested to try to obtain the electronic spectra of these two transient species to further assess this proposed mechanism of formation of CPO-I.

Acknowledgment. Support for this work from a National Science Foundation Grant (MCB-9817028) and a NATO Collaborative Research Grant (CRG931521) is gratefully acknowledged. The authors also gratefully acknowledge use of the T-3D machine at the Pittsburgh Supercomputing Center under NSF grant MCA93S007P.

JA993000B

(18) Filizola, M.; Loew, G. *J. Am. Chem. Soc.* **2000**, *122* (1), 18–25.